

Focus Your Attention: Towards Data-Intuitive Lightweight Vision Transformers

Suyash Gaurav *
Tokyo International University
Tokyo, Japan

Muhammad Farhan Humayun *
University of Turku
Turku, Finland

Jukka Heikkonen
University of Turku
Turku, Finland

Jatin Chaudhary
University of Turku
Turku, Finland
jatin.chaudhary@utu.fi

Abstract

The evolution of Vision Transformers has led to their widespread adaptation to different domains. Despite large-scale success, there remain significant challenges including their reliance on extensive computational and memory resources for pre-training on huge datasets as well as difficulties in task-specific transfer learning. These limitations coupled with energy inefficiencies mainly arise due to the computation-intensive self-attention mechanism. To address these issues, we propose a novel **Super-Pixel Based Patch Pooling (SPPP)** technique that generates context-aware, semantically rich, patch embeddings to effectively reduce the architectural complexity and improve efficiency. Additionally, we introduce the **Light Latent Attention (LLA)** module in our pipeline by integrating latent tokens into the attention mechanism allowing cross-attention operations to significantly reduce the time and space complexity of the attention module. By leveraging the data-intuitive patch embeddings coupled with dynamic positional encodings, our approach adaptively modulates the cross-attention process to focus on informative regions while maintaining the global semantic structure. This targeted attention improves training efficiency and accelerates convergence. Notably, the SPPP module is lightweight and can be easily integrated into existing transformer architectures. Extensive experiments demonstrate that our proposed architecture provides significant improvements in terms of computational efficiency while achieving comparable results with the state-of-the-art approaches, highlighting its potential for energy-efficient transformers suitable for edge deployment. (The code is available on our GitHub repository: <https://github.com/zser092/Focused-Attention-ViT>).

1 Introduction

The self-attention mechanism which forms the core of the transformer architecture was originally designed to handle a variety of Natural Language Processing (NLP) tasks such as machine translation Vaswani et al. [2017], sentiment classification Lin et al. [2017], Ambartsoumian and Popowich [2018] sentence prediction Devlin et al. [2018] reading comprehension Yang et al. [2019] etc. The mechanism has been further adapted to advanced reasoning models such as Generative Pretrained Transformer (GPT) Radford and Narasimhan [2018] and DeepSeek et. al. [2025]. The principal

*These authors contributed equally and share first authorship.

advantage of the self-attention mechanism is its ability to effectively capture the long-range dependencies more efficiently as compared to its old rival i.e. the recurrent neural networks (RNNs). Concretely, self-attention enables the model to weigh the relevance of different tokens in a sequence relative to each other, regardless of their position.

The adaptation of this approach towards Computer Vision tasks, first proposed by Dosovitskiy et.al, Dosovitskiy et al. [2021] allows the processing of 2D input image patches in a similar fashion compared to the word tokens in NLP tasks. Figure 1 illustrates this process in Vision Transformers (ViT) from the input image to the patch embeddings which are directly passed on to the multi-head self-attention modules. To exemplify, we use a resampled goldfish image from the ImageNet dataset to show the intermediate outputs generated during the embedding process. Considering the input image is: $\mathbf{X} \in \mathbb{R}^{H \times W \times C}$.

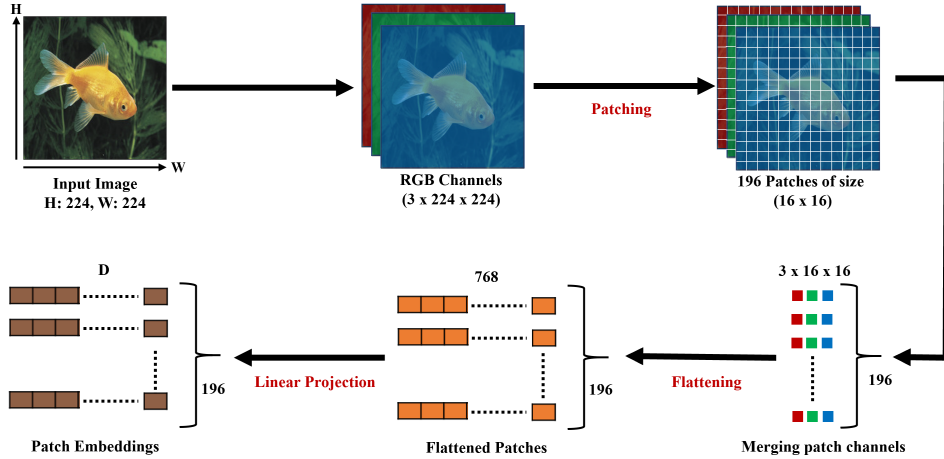


Figure 1: Illustration of the Patch Embedding Module for Vision Transformers

In the provided example, the input image is resampled to 224 x 224 pixels and contains 3 color channels. It is then divided into 196 equal sized, non-overlapping patches of 16 x 16 using the following equation:

$$N = \frac{H \times W}{P^2} \quad (1)$$

Here, N denotes the number of patches (excluding the class token), H and W correspond to the height and width of the input image, respectively, and P is the side length of each square patch (i.e., assuming square patches of size $P \times P$).

Each patch is flattened to form a vector, $\mathbf{x}_i \in \mathbb{R}^{P^2 \cdot C}$, for $i = 1, \dots, N$. In the provided example, we have 196 different vectors of size $16 \times 16 \times 3 = 768$. Each flattened patch vector \mathbf{x}_i is projected to a lower-dimensional embedding space using a learnable linear transformation: $\mathbf{E} \in \mathbb{R}^{(P^2 \cdot C) \times D}$, where D is the transformer embedding dimension:

$$\mathbf{z}_i = \mathbf{x}_i \mathbf{E} \in \mathbb{R}^D \quad (2)$$

A key observation here is that the number of final patch embeddings scales linearly with the number of input image patches which in turn depends on the input image resolution and the individual patch size. In the subsequent multi-headed self-attention, each patch embedding is correlated against one another resulting in quadratic complexity i.e., $O(N^2)$. Considering the example as illustrated in Figure 1, there are 196 patch embeddings which amount to $(196)^2 \approx 38k$ pairwise correlation computations within the self-attention module.

We introduce robust techniques to effectively reduce the embedding dimensions by intelligently fusing the input patches based on the inherent semantic structure. This in turn reduces the computational overhead of the self-attention module, while preserving and propagating rich semantic information to the deeper layers of the network to facilitate convergence and more efficient training. The main contributions of our work are as follows:

- We propose the novel Super-Pixel Based Patch Pooling (SPPP) algorithm to intelligently reduce the number of patch embeddings which are fed into the attention mechanism by merging the input image patches based on their intrinsic semantic properties.
- We propose replacing the multi-headed attention modules with the **novel** Light Latent Attention (LLA) mechanism in the ViT architecture, enabling efficient cross-attention operations with latent tokens.
- Our architectural modifications significantly reduce the time and space complexity of the attention mechanism which is the major bottleneck in the ViT architecture in terms of computational and temporal requirements.
- We conduct extensive experiments and ablation studies on various public benchmark datasets to validate the effectiveness of our proposed techniques.

2 Background and Related Work

Vision Transformers (ViTs) have shown remarkable success across various tasks from image classification Dosovitskiy et al. [2021], Touvron et al. [2021], Liu et al. [2021], Wang et al. [2025] to more complex tasks including segmentation, Zheng et al. [2021], Xie et al. [2021], YUAN et al. [2021], Thisanke et al. [2023] object detection, Carion et al. [2020], Liu et al. [2022a], Zhao et al. [2024], Zhang et al. [2025] and video understanding Arnab et al. [2021], Bertasius et al. [2021], Chen et al. [2024]. Similarly, a large number of domain-specific studies utilizing transformer architectures also exist, such as medical image analysis Hatamizadeh et al. [2022], He et al. [2023], Aburass et al. [2025], remote sensing Hong et al. [2022], Yao et al. [2023], pose estimation Li et al. [2023] and action recognition Ahn et al. [2023] etc. Since the groundbreaking approach of replacing the traditional convolutional operations entirely with attention-based architectures proposed by Dosovitskiy et al. [2021], the ViT architecture has been studied vastly proposing improved, more robust variants of the originally proposed model. For instance, to mitigate the heavy computational burden, several works have proposed architectural modifications aimed at improving efficiency. DeiT Touvron et al. [2021] introduced knowledge distillation to train ViTs on smaller datasets without sacrificing accuracy. T2T-ViT Yuan et al. [2021] employed a tokens-to-token transformation that progressively aggregates information before applying self-attention. Similarly, MobileViT Mehta and Rastegari [2022] integrated convolutions into the transformer pipeline to enhance locality and reduce computational cost, making ViTs more viable for mobile settings. Other works like PoolFormer Yu et al. [2022] and PiT Heo et al. [2021] introduced hierarchical token reduction strategies and spatial pooling mechanisms to reduce input sequence length progressively. LeViT Graham et al. [2021] leveraged downsampling and hybrid convolutions to strike a better latency-accuracy trade-off. These variants highlight a trend toward building lightweight and scalable ViTs, but they often compromise the richness of patch representations or spatial context.

The self-attention mechanism scales quadratically with input sequence length. To address this, Linformer Wang et al. [2020] approximated self-attention with low-rank projections, while Nystromformer Xiong et al. [2021] introduced kernel-based and landmark-based approximations. Swin Transformer Liu et al. [2021] introduced a hierarchical architecture with shifted window attention to improve scalability and efficiency in vision tasks. Its successor, Swin Transformer V2 Liu et al. [2022b], further enhanced training stability and generalization through log-scaled relative position bias and scaled cosine attention, enabling deployment at a billion-parameter scale. Light Vision Transformer Yang et al. [2022] proposed separate enhanced self-attention mechanisms for low and high-level features to improve efficiency. DynamicViT Rao et al. [2021] proposed learning to prune tokens during inference, enabling adaptive computation without retraining. CrossViT Chen et al. [2021] demonstrated the value of multi-scale token fusion using cross-attention, whereas other works like TokenLearner Ryoo et al. [2021] and AdaViT Meng et al. [2022] introduced dynamic token selection and routing to focus computation on informative regions, similar in spirit to the dynamic attention strategy we explore. ShiftAddViT You et al. [2023] reduces the computational cost of Vision Transformers by reparameterizing attention and MLPs using shift and addition operations, enabling significant GPU latency and energy savings without retraining from scratch. More recently, Look Here Vision Transformer Fuller et al. [2024] proposed a novel position encoding method via 2D attention masks to improve translation equivariance and attention head diversity. Similarly, MicroViT proposed Setyawan et al. [2025] an efficient single-head attention mechanism to reduce the computational complexity of the overall ViT architecture.

Superpixels have been leveraged for context-aware representations in traditional vision tasks, but their integration into transformers remains underexplored. Superpixel-based attention Zhu et al. [2023] and patch grouping strategies have shown promise in enhancing spatial coherence while reducing token count. Our proposed SPPP module builds on this insight by using semantically aligned patch pooling to guide attention and reduce computational overhead.

3 Methodology

In this section, we discuss the proposed architectural changes to the ViT in detail. Figure 2 demonstrates the key differences of the proposed architecture compared with the original ViT. The first major difference is that the regular, fixed grid patch embedding module is replaced by our newly proposed, dynamic SPPP module which generates compact, high-semantic embeddings. The second key difference is the modification in the attention module. The regular multi-head attention module is replaced by the novel LLA which uses latent tokens to reduce the computational overhead of the attention module, making the overall architecture light-weight. The details of the newly proposed modules are discussed in the following sub-sections.

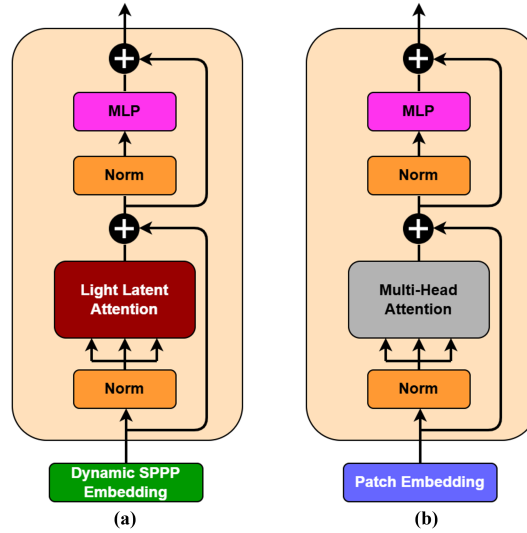


Figure 2: Key architectural differences: (a) Proposed ViT with Focused Attention, (b) Original ViT.

3.1 Super-Pixel Based Patch Pooling (SPPP)

The main idea proposed in the SPPP module is to generate dynamic and semantically rich patch embeddings instead of the regular static embeddings used in the ViT. Figure 3 provides an overview of the various steps involved in the SPPP module.

Let us break down the SPPP module. First, we divide the input image into regular equal-sized patches according to the criteria mentioned in Eq. 1. In parallel, we apply the Simple Linear Iterative Clustering (SLIC) algorithm Achanta et al. [2012], to group the input image into regions with coherent semantic properties called Super-pixels. This can be conceptualized as puzzle pieces that naturally follow the semantic features such as color, texture and edges etc. and typically comprise a meaningful part of the scene. The SLIC performs searching in a fixed search space grid of $2S \times 2S$ to improve computational efficiency, such that:

$$S = \sqrt{\left(\frac{N}{K}\right)} \quad (3)$$

Here, S is the sampling interval, N is the number of pixels in the image, and K is the number of clusters. The strength of the SLIC algorithm is that it performs clustering in 5D space combining the

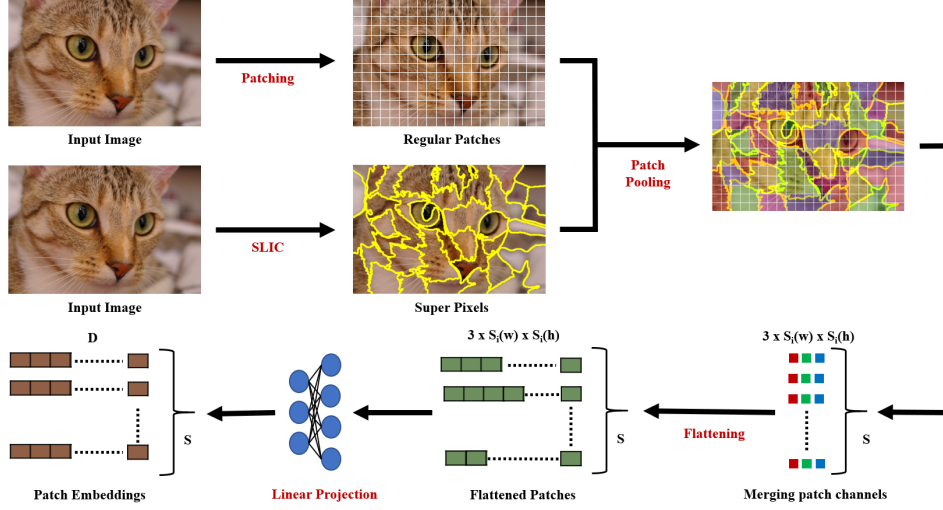


Figure 3: Workflow of the SPPP module.

distance measures in color and spatial dimensions into a single metric using the following equation:

$$D = \sqrt{(d_c)^2 + \left(\frac{d_s}{S}\right)^2 m^2} \quad (4)$$

Here, d_c is the distance in color space, d_s is the spatial distance, and m is the compactness factor which balances color similarity and spatial proximity. A larger value of m means that more importance is given to spatial proximity, whereas a lower value of m signifies more value for color and tone similarity. Once we have the initial super-pixels from the SLIC algorithm, we overlay the regular patch grids on the super-pixels and compute the overlap of all the patches with corresponding super-pixels. The following equation sums up this operation:

$$O_{i,j} = \frac{|S_i \cap P_j|}{|P_j|} = \frac{\sum_{(x,y) \in P_j} \mathbf{1}((x,y) \in S_i)}{16 \times 16} \quad (5)$$

Here, S_i is the i^{th} super-pixel produced by the SLIC algorithm, P_j is the j^{th} regular patch from the grid (e.g., 16×16 patch size), $S_i \cap P_j$ is the overlap region between the i^{th} super-pixel and the j^{th} regular patch, $|P_j|$ is the area (number of pixels) of the regular patch, here assumed to be 16×16 . The indicator function $\mathbf{1}((x,y) \in S_i)$ equals 1 if the pixel at (x,y) belongs to super-pixel S_i and 0 otherwise. We merge patches j,k if there exists an i such that both $O_{i,j}$ and $O_{i,k}$ exceed a threshold τ .

Finally, we proceed by flattening the RGB color channels corresponding to each super patch to form flattened vectors. It is worth noting that in our case since the size of each super patch varies, our flattened vectors also have varying lengths depending on the number of pixels included in the corresponding super patches. The flattened patch vectors are then linearly projected to fixed-sized super-patch embeddings as demonstrated in Figure 3. This gives us one embedding per super patch, rather than many small, noisy patch embeddings. It is also notable that the number of final super patch embeddings S , each representing a meaningful region of the image is considerably less as compared to the initial patch embeddings N as shown in Figure 1, which in turn leads to less FLOPS and hence, improved spatial and temporal computational efficiency.

To preserve the spatial awareness with respect to the super patch embeddings, we compute new dynamic positional encodings that are consistent with the reduced set of tokens based on the centroid of each super-pixel such that:

$$c_x^r = \frac{1}{|S_r|} \sum_{(x,y) \in S_r} x, \quad c_y^r = \frac{1}{|S_r|} \sum_{(x,y) \in S_r} y,$$

then:

$$PE_r = \text{MLP} \left(\frac{c_x^r}{W}, \frac{c_y^r}{H} \right) \in \mathbb{R}^D,$$

Here, S_r denotes the set of pixels belonging to the r^{th} super-pixel and $|S_r|$ is the number of pixels in S_r , i.e., the cardinality of the set. The variables (x, y) represent pixel coordinates within S_r , while c_x^r and c_y^r are the x- and y-coordinates of the centroid of superpixel S_r , respectively. The terms W and H refer to the width and height of the input image in pixels. The expressions c_x^r/W and c_y^r/H correspond to the normalized centroid coordinates in the range $[0, 1]$. The function MLP denotes a Multi-Layer Perceptron, which maps these normalized coordinates to a positional encoding vector $PE_r \in \mathbb{R}^D$, where D is the embedding dimension used in the transformer model.

Following the flattening stage, to maintain spatial coherence in the reduced token representation derived from super-pixels, we introduce dynamic positional encodings anchored to the geometric centroids of each super-pixel region. For a given super-pixel S_r , the centroid coordinates (c_x^r, c_y^r) are computed as the mean of the pixel coordinates contained within the region. These coordinates are subsequently normalized by the image dimensions W and H , and projected into the embedding space \mathbb{R}^D via a multilayer perceptron (MLP). The resulting positional encoding PE_r is then added to the corresponding super patch embedding. This approach enables the model to retain spatial contextuality in a manner that aligns with the underlying image structure, as defined by the super-pixel segmentation, rather than relying on fixed-grid positional priors.

Algorithm 1 Superpixel-based Patch Pooling (SPPP)

Require: Image \mathcal{I} , patch size $p \times p$, number of superpixels K

Ensure: Superpixel-level embeddings $\{h_i\}_{i=1}^K$

- 1: Partition \mathcal{I} into fixed-size patches $\{P_j\}$
 - 2: Apply SLIC to compute K superpixels $\{S_i\}$
 - 3: **for** each superpixel S_i **do**
 - 4: Compute overlap between S_i and all patches $\{P_j\}$
 - 5: Aggregate patch features using overlap weights to form h_i
 - 6: Compute centroid $(c_{i,x}, c_{i,y})$ of S_i
 - 7: Normalize centroid with image dimensions
 - 8: Compute positional encoding via MLP
 - 9: Add positional encoding to h_i
 - 10: **end for**
 - 11: **return** Super patch embeddings $\{h_i\}$
-

3.2 Light Latent Attention (LLA)

We propose the LLA module to further reduce the dimensions of the embedding vectors using the concept of latent tokens. Figure4 illustrates the overall architecture of the LLA module.

As shown in the Figure4, h_i are the patch embeddings vector, where $h_i \in \mathbb{R}^{X \times D}$. Moving forward into the LLA module, the Key and Value vector h_i^{KV} is separately reshaped into appropriate Key and Value tensors based on the length of the input sequence, the number of attention heads and the dimensions of each head. On the other hand, we perform low rank compression of the Query vectors through learned projection matrices to generate latent representations c_t^Q et. al. [2024], where $c_t^Q \in \mathbb{R}^{L \times D}$. It is worth noting that ($L \ll X$). This compression is aimed to reduce memory consumption during model training. After that, the Query tensor derived from the latent representation and the Key and Value tensors derived from the original input are fed into the attention module to carry out cross-attention operations. The overall computations of the LLA module are summarized by following equations:

$$Q = c_t^Q W_Q \in \mathbb{R}^{B \times L \times D} \quad (6)$$

$$K = h_i W_K \in \mathbb{R}^{B \times X \times D}, V = h_i W_V \in \mathbb{R}^{B \times X \times D} \quad (7)$$

where $W_Q, W_K, W_V \in \mathbb{R}^{D \times D}$ are learned projection matrices, B is the batch size and L, X are lengths of latent tokens and input sequences respectively.

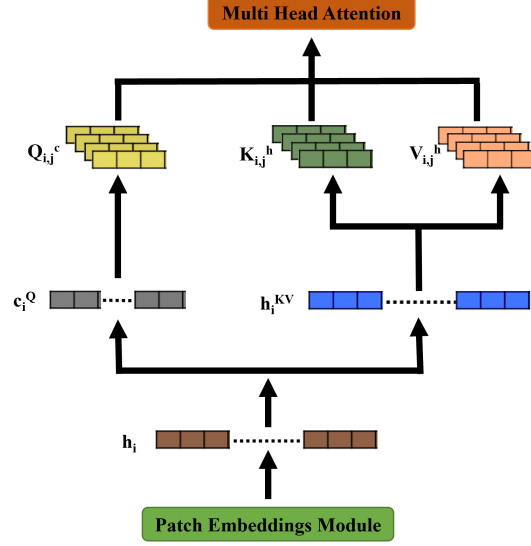


Figure 4: Architecture of the LLA module.

The K, Q and V are further reshaped to split them for feeding into multiple heads as follows:

$$\mathbf{Q} \rightarrow \mathbb{R}^{B \times H \times L \times d}, \mathbf{K}, \mathbf{V} \rightarrow \mathbb{R}^{B \times H \times T \times d} \quad (8)$$

Where H is the number of heads such that $d = D/H$. Finally we compute the scaled dot product cross-attention across the latent Query vectors and the input projected Key and Values vectors as follows:

$$\mathbf{A}_{b,h} = \text{softmax} \left(\frac{\mathbf{Q}_{b,h} \mathbf{K}_{b,h}^\top}{\sqrt{d}} \right) \in \mathbb{R}^{L \times X} \quad (9)$$

$$\mathbf{O}_{b,h} = \mathbf{A}_{b,h} \mathbf{V}_{b,h} \in \mathbb{R}^{L \times d} \quad (10)$$

Outputs of the multiple heads are concatenated and progressed to the further layers of the model.

Algorithm 2 Light Latent Attention (LLA)

Require: Superpixel embeddings $\{h_i\}$ from SPPP

Ensure: Attention-enhanced embeddings $\{z_i\}$

- 1: **for** each embedding h_i **do**
 - 2: Apply layer normalization to obtain \tilde{h}_i
 - 3: Split \tilde{h}_i into latent query and key-value components
 - 4: Project components to form Q_i , K_i , and V_i
 - 5: Compute attention output using multi-head attention
 - 6: **end for**
 - 7: **return** Computed Attentions
-

4 Experimental Setup

4.1 Implementation Details

Table 1 shows different parameters comparing the base ViT architecture to our proposed Focused attention ViT. We intend to keep the architecture of our proposed model as close as possible to the original ViT while reducing the computational complexity of the attention mechanism through a combination of the SPPP and LLA modules. Regarding the training parameters, we consistently use the AdamW stochastic optimizer with a learning rate of 1×10^{-4} , batch size of 128 and a weight decay of 0.05 throughout our experiments. We train all the models for 50 epochs on respective datasets. For experiments involving pretrained weights, we use ImageNet weights trained using the

Table 1: Comparison of the Base ViT model with our proposed Focused attention ViT.

Component	Base ViT	Focused attention ViT
Patch Size	4×4	4×4
Embedding Dimension	768	768
Transformer Layers	12	12
Attention Heads	12	12
FFN Dimensions	768	768
No. of final patches	N	S (where $S < N$)
Positional Encoding	Learned Fixed Grid	Learned Dynamic (Super-pixel Centroids)
Latent Token Dimensions	—	L (where $L \ll N$)

original ViT model. All the experiments were carried out on a local machine using Intel Core i9 14900HX processor, NVIDIA RTX 4090 GPU (24 GB VRAM, ~ 82 TFLOPS FP32) and 64 GB DDR4 RAM. For evaluation metrics, we use parameters such as accuracy(%), training time, inference speed(secs/image) and memory consumption(GBs) to assess the performance of all the models.

4.2 Datasets

We use five different datasets to train our models for carrying our comparative analysis including CIFAR-10, CIFAR-100 Krizhevsky [2012], SVHN Netzer et al. [2011], Fashion MNIST Xiao et al. [2017] and STL10 Coates et al. [2011]. Due to their low image dimensions, these datasets serve an ideal purpose to perform rapid experimental evaluation for the transformer-based architectures. The details of these datasets are included in the appendix.

4.3 Results

We train eight distinct models across all datasets, including the baseline Vision Transformer (ViT) initialized with both random and pre-trained weights. One variant, termed Cross-Attention ViT, employs a simplified cross-attention mechanism where the attention operates between compressed feature representations and the original patch embeddings. To enhance this further, the Multi-Head Cross-Attention ViT extends the mechanism across multiple attention heads, enabling the model to attend to diverse subspaces of the compressed features simultaneously. Finally, we evaluate our proposed Focused Attention ViT, which incorporates the SPPP and LLA modules to more effectively guide the attention process toward salient regions. The experimental results are summarized in Tables 3–6. The last three rows of each table represent the ablation experiments of our proposed Focused Attention ViT. Table 2 reports the training times for all models. The standard ViT with random initialization exhibits the highest training times across all datasets. In contrast, the Cross-Attention and Multi-Head Cross-Attention ViTs achieve modest improvements in efficiency. The ViT model initialized with pre-trained weights converges significantly faster than its randomly initialized counterparts. Notably, our proposed Focused Attention ViT including SPPP and LLA modules achieves the greatest efficiency, reducing training times by more than 45% across all datasets.

Table 2: Training Time (mins)

Model	CIFAR-10	CIFAR-100	SVHN	FashionMNIST	STL-10
ViT	186.67	202.85	275.00	225.00	78.33
Pretrained ViT	74.67	81.10	110.00	90.00	31.33
Cross-Attention ViT	171.67	186.33	251.67	206.67	72.33
Multi-Head Cross ViT	161.00	173.45	235.00	193.33	66.83
ViT + SPPP	97.67	106.92	143.17	117.17	39.00
Pretrained ViT + SPPP	39.00	42.80	57.33	46.83	15.67
Pretrained ViT + LLA	50.70	55.98	74.53	60.88	17.23
Pretrained ViT + SPPP + LLA	38.42	41.77	56.85	46.29	15.34

Table3 shows the performance of all models in terms of the percentage accuracy achieved. The pre-trained ViT achieves the best accuracy values overall. Focused attention ViT also achieves comparative accuracy values but with significantly lower training times as mentioned in Table1.

Table 3: Accuracy (%) (All results within ± 0.5 threshold)

Model	CIFAR10	CIFAR100	SVHN	FashionMNIST	STL10
ViT	95.4	81.2	96.7	92.3	90.5
Pretrained ViT	96.7	82.3	97.8	93.3	91.6
Cross-Attention ViT	95.6	80.7	96.5	92.2	90.4
Multi-Head Cross ViT	95.8	81.0	96.8	92.4	90.6
ViT + SPPP	94.3	79.0	95.5	91.0	89.1
Pretrained ViT + SPPP	95.7	80.3	96.6	92.1	90.3
Pretrained ViT + LLA	96.0	81.2	96.9	92.6	90.8
Pretrained ViT + SPPP + LLA	95.9	80.9	96.7	92.5	90.7

Similarly, Table4 shows the memory consumption of each model with respect to different datasets. The proposed Focused attention ViT has approximately 90% less memory consumption as compared to the other models signifying its light-weight abilities. Finally, Table5 shows the inference times taken per image for all the datasets included in the study. It can be seen that due to the light-weight architecture of our newly proposed model, it has the fastest inference times compared to other models as well.

Table 4: Memory Usage (GBs) during Training

Model	CIFAR-10	CIFAR-100	SVHN	FashionMNIST	STL-10
ViT	5.3	5.6	5.2	5.1	17.4
Pretrained ViT	5.1	5.4	5.0	5.0	16.8
Cross-Attention ViT	4.2	4.5	4.1	4.0	13.5
Multi-Head Cross ViT	4.6	4.9	4.4	4.3	14.2
ViT + SPPP	0.42	0.45	0.40	0.39	0.72
Pretrained ViT + SPPP	0.41	0.44	0.39	0.38	0.71
Pretrained ViT + LLA	0.50	0.54	0.47	0.46	0.85
Pretrained ViT + SPPP + LLA	0.39	0.43	0.37	0.36	0.67

Table 5: Inference Time (secs/image)

Model	CIFAR-10	CIFAR-100	SVHN	FashionMNIST	STL-10
ViT	0.102	0.106	0.098	0.094	1.12
Pretrained ViT	0.097	0.102	0.092	0.089	1.08
Cross-Attention ViT	0.090	0.095	0.088	0.085	1.00
Multi-Head Cross ViT	0.083	0.089	0.081	0.078	0.95
ViT + SPPP	0.048	0.052	0.046	0.043	0.21
Pretrained ViT + SPPP	0.045	0.050	0.043	0.041	0.19
Pretrained ViT + LLA	0.064	0.069	0.061	0.059	0.36
Pretrained ViT + SPPP + LLA	0.043	0.047	0.041	0.039	0.18

5 Discussion and Conclusion

As demonstrated by our experimental results, our proposed Focused Attention ViT significantly improves the computational efficiency including training time, memory usage and inference speed while maintaining comparable accuracy to the original ViT. These improvements are achieved by incorporating the SPPP and LLA modules in the ViT. The SPPP module implements the strategy of adaptive spatial pooling of the patches based on super-pixel clustering to generate semantically meaningful super patches. This approach yields rich patch embedding with less number of embedding

vectors compared to the original ViT. Effectively, the SPPP module reduces the space complexity of the ViT architecture from $\mathcal{O}(N^2)$ to $\mathcal{O}(S^2)$, where $S < N$. The LLA module further enhances the efficiency by reducing the set of Query vectors through intermediate learnable latent tokens before passing them to the attention heads. The LLA reduces the complexity $\mathcal{O}(S^2)$ to $\mathcal{O}(L \times S)$, where $L \ll S$. Therefore, both modules play their part in effectively reducing the embedding tokens while retaining useful feature information necessary to train the model. This results in a considerable reduction in the computational overhead of the attention mechanism making the overall ViT architecture more robust and light-weight.

In conclusion, the computationally intensive nature of the self-attention mechanism poses significant challenges for deploying ViT-based architectures on high-resolution images under resource-constrained settings. Similarly, training convergence for ViTs is also difficult due to the requirement of huge training datasets. To address these issues, we proposed the Focused Attention ViT by introducing two novel modules called SPPP and LLA. These modules collectively improve the computational performance of the ViT architecture by leveraging the inherent semantic structure of the input images and generating learnable latent token representations respectively. Our results demonstrate substantial improvements in model training times, inference speed and memory efficiency while achieving comparable accuracy with the standard ViT model. This work is a continuation of the efforts toward the development of efficient and robust ViT-based architectures that have the possibility of being implemented on edge devices under real-time settings. We are excited about the future prospects of this work in developing resource-friendly and data-efficient models. In future, we plan to explore the possibility and impact of using a latent-heavy implementation of the attention mechanism in the ViT architecture as well as testing our results on more complex datasets with larger image dimensions.

References

- Sanad Aburass, Osama Dorgham, Jamil Al Shaqsi, Maha Abu Rumman, and Omar Al-Kadi. Vision transformers in medical imaging: a comprehensive review of advancements and applications across multiple diseases. *Journal of Imaging Informatics in Medicine*, Mar 2025. ISSN 2948-2933. doi: 10.1007/s10278-025-01481-y. URL <https://doi.org/10.1007/s10278-025-01481-y>.
- Radhakrishna Achanta, Appu Shaji, Kevin Smith, Aurelien Lucchi, Pascal Fua, and Sabine Süsstrunk. Slic superpixels compared to state-of-the-art superpixel methods. *IEEE Transactions on Pattern Analysis and Machine Intelligence*, 34(11):2274–2282, 2012. doi: 10.1109/TPAMI.2012.120.
- Dasom Ahn, Sangwon Kim, Hyunsu Hong, and Byoung Chul Ko. Star-transformer: A spatio-temporal cross attention transformer for human action recognition. In *2023 IEEE/CVF Winter Conference on Applications of Computer Vision (WACV)*, pages 3319–3328, 2023. doi: 10.1109/WACV56688.2023.00333.
- Artaches Ambartsoumian and Fred Popowich. Self-attention: A better building block for sentiment analysis neural network classifiers. In Alexandra Balahur, Saif M. Mohammad, Veronique Hoste, and Roman Klinger, editors, *Proceedings of the 9th Workshop on Computational Approaches to Subjectivity, Sentiment and Social Media Analysis*, pages 130–139, Brussels, Belgium, October 2018. Association for Computational Linguistics. doi: 10.18653/v1/W18-6219. URL <https://aclanthology.org/W18-6219/>.
- Anurag Arnab, Mostafa Dehghani, Georg Heigold, Chen Sun, Mario Lučić, and Cordelia Schmid. Vivit: A video vision transformer. In *2021 IEEE/CVF International Conference on Computer Vision (ICCV)*, pages 6816–6826, 2021. doi: 10.1109/ICCV48922.2021.00676.
- Gedas Bertasius, Heng Wang, and Lorenzo Torresani. Is space-time attention all you need for video understanding? In Marina Meila and Tong Zhang, editors, *Proceedings of the 38th International Conference on Machine Learning*, volume 139 of *Proceedings of Machine Learning Research*, pages 813–824. PMLR, 18–24 Jul 2021. URL <https://proceedings.mlr.press/v139/bertasius21a.html>.
- Nicolas Carion, Francisco Massa, Gabriel Synnaeve, Nicolas Usunier, Alexander Kirillov, and Sergey Zagoruyko. End-to-end object detection with transformers. In *Computer Vision – ECCV 2020: 16th European Conference, Glasgow, UK, August 23–28, 2020, Proceedings, Part I*, page 213–229, Berlin, Heidelberg, 2020. Springer-Verlag. ISBN 978-3-030-58451-1. doi: 10.1007/978-3-030-58452-8_13. URL https://doi.org/10.1007/978-3-030-58452-8_13.

- Chun-Fu Richard Chen, Quanfu Fan, and Rameswar Panda. Crossvit: Cross-attention multi-scale vision transformer for image classification. In *2021 IEEE/CVF International Conference on Computer Vision (ICCV)*, pages 347–356, 2021. doi: 10.1109/ICCV48922.2021.00041.
- Dong Chen, Peisong Wu, Mingdong Chen, Mengtao Wu, Tao Zhang, and Chuanqi Li. Ls-vit: Vision transformer for action recognition based on long and short-term temporal difference. *Frontiers in Neurorobotics*, 18, 10 2024. doi: 10.3389/fnbot.2024.1457843.
- Adam Coates, Andrew Ng, and Honglak Lee. An analysis of single-layer networks in unsupervised feature learning. In Geoffrey Gordon, David Dunson, and Miroslav Dudík, editors, *Proceedings of the Fourteenth International Conference on Artificial Intelligence and Statistics*, volume 15 of *Proceedings of Machine Learning Research*, pages 215–223, Fort Lauderdale, FL, USA, 11–13 Apr 2011. PMLR. URL <https://proceedings.mlr.press/v15/coates11a.html>.
- Jacob Devlin, Ming-Wei Chang, Kenton Lee, and Kristina Toutanova. BERT: pre-training of deep bidirectional transformers for language understanding. *CoRR*, abs/1810.04805, 2018. URL <http://arxiv.org/abs/1810.04805>.
- Alexey Dosovitskiy, Lucas Beyer, Alexander Kolesnikov, Dirk Weissenborn, Xiaohua Zhai, Thomas Unterthiner, Mostafa Dehghani, Matthias Minderer, Georg Heigold, Sylvain Gelly, Jakob Uszkoreit, and Neil Houlsby. An image is worth 16x16 words: Transformers for image recognition at scale. In *9th International Conference on Learning Representations, ICLR 2021, Virtual Event, Austria, May 3-7, 2021*. OpenReview.net, 2021. URL <https://openreview.net/forum?id=YicbFdNTTy>.
- Aixin Liu et. al. Deepseek-v2: A strong, economical, and efficient mixture-of-experts language model, 2024. URL <https://arxiv.org/abs/2405.04434>.
- Aixin Liu et. al. Deepseek-v3 technical report, 2025. URL <https://arxiv.org/abs/2412.19437>.
- Anthony Fuller, Daniel Kyrollos, Yousef Yassin, and James R Green. Lookhere: Vision transformers with directed attention generalize and extrapolate. In *The Thirty-eighth Annual Conference on Neural Information Processing Systems*, 2024. URL <https://openreview.net/forum?id=o7D0GbZeyP>.
- Ben Graham, Alaaeldin El-Nouby, Hugo Touvron, Pierre Stock, Armand Joulin, Hervé Jégou, and Matthijs Douze. Levit: a vision transformer in convnet’s clothing for faster inference. In *2021 IEEE/CVF International Conference on Computer Vision (ICCV)*, pages 12239–12249, 2021. doi: 10.1109/ICCV48922.2021.01204.
- Ali Hatamizadeh, Yucheng Tang, Vishwesh Nath, Dong Yang, Andriy Myronenko, Bennett Landman, Holger R. Roth, and Daguang Xu. Unetr: Transformers for 3d medical image segmentation. In *2022 IEEE/CVF Winter Conference on Applications of Computer Vision (WACV)*, pages 1748–1758, 2022. doi: 10.1109/WACV51458.2022.00181.
- Kelei He, Chen Gan, Zhuoyuan Li, Islem Rekik, Zihao Yin, Wen Ji, Yang Gao, Qian Wang, Junfeng Zhang, and Dinggang Shen. Transformers in medical image analysis. *Intelligent Medicine*, 3(1):59–78, 2023. ISSN 2667-1026. doi: <https://doi.org/10.1016/j.imed.2022.07.002>. URL <https://www.sciencedirect.com/science/article/pii/S2667102622000717>.
- Byeongho Heo, Sangdoo Yun, Dongyoon Han, Sanghyuk Chun, Junsuk Choe, and Seong Joon Oh. Rethinking spatial dimensions of vision transformers. In *2021 IEEE/CVF International Conference on Computer Vision (ICCV)*, pages 11916–11925, 2021. doi: 10.1109/ICCV48922.2021.01172.
- Danfeng Hong, Zhu Han, Jing Yao, Lianru Gao, Bing Zhang, Antonio Plaza, and Jocelyn Chanussot. Spectralformer: Rethinking hyperspectral image classification with transformers. *IEEE Transactions on Geoscience and Remote Sensing*, 60:1–15, 2022. doi: 10.1109/TGRS.2021.3130716.
- Alex Krizhevsky. Learning multiple layers of features from tiny images. *University of Toronto*, 05 2012.
- Wenhao Li, Hong Liu, Runwei Ding, Mengyuan Liu, Pichao Wang, and Wenming Yang. Exploiting temporal contexts with strided transformer for 3d human pose estimation. *IEEE Transactions on Multimedia*, 25:1282–1293, 2023. doi: 10.1109/TMM.2022.3141231.

- Zhouhan Lin, Minwei Feng, Cícero Nogueira dos Santos, Mo Yu, Bing Xiang, Bowen Zhou, and Yoshua Bengio. A structured self-attentive sentence embedding. *CoRR*, abs/1703.03130, 2017. URL <http://arxiv.org/abs/1703.03130>.
- Shilong Liu, Feng Li, Hao Zhang, Xiao Yang, Xianbiao Qi, Hang Su, Jun Zhu, and Lei Zhang. DAB-DETR: Dynamic anchor boxes are better queries for DETR. In *International Conference on Learning Representations*, 2022a. URL <https://openreview.net/forum?id=oMI9Pj0b9Jl>.
- Ze Liu, Yutong Lin, Yue Cao, Han Hu, Yixuan Wei, Zheng Zhang, Stephen Lin, and Baining Guo. Swin transformer: Hierarchical vision transformer using shifted windows. In *2021 IEEE/CVF International Conference on Computer Vision (ICCV)*, pages 9992–10002, 2021. doi: 10.1109/ICCV48922.2021.00986.
- Ze Liu, Han Hu, Yutong Lin, Zhuliang Yao, Zhenda Xie, Yixuan Wei, Jia Ning, Yue Cao, Zheng Zhang, Li Dong, Furu Wei, and Baining Guo. Swin transformer v2: Scaling up capacity and resolution. In *2022 IEEE/CVF Conference on Computer Vision and Pattern Recognition (CVPR)*, pages 11999–12009, 2022b. doi: 10.1109/CVPR52688.2022.01170.
- Sachin Mehta and Mohammad Rastegari. Mobilevit: Light-weight, general-purpose, and mobile-friendly vision transformer. In *International Conference on Learning Representations*, 2022. URL <https://openreview.net/forum?id=vh-0sUt8HlG>.
- Lingchen Meng, Hengduo Li, Bor-Chun Chen, Shiyi Lan, Zuxuan Wu, Yu-Gang Jiang, and Ser-Nam Lim. Advait: Adaptive vision transformers for efficient image recognition. In *2022 IEEE/CVF Conference on Computer Vision and Pattern Recognition (CVPR)*, pages 12299–12308, 2022. doi: 10.1109/CVPR52688.2022.01199.
- Yuval Netzer, Tao Wang, Adam Coates, Alessandro Bissacco, Bo Wu, and Andrew Ng. Reading digits in natural images with unsupervised feature learning. *NIPS*, 01 2011.
- Alec Radford and Karthik Narasimhan. Improving language understanding by generative pre-training. 2018. URL <https://api.semanticscholar.org/CorpusID:49313245>.
- Yongming Rao, Wenliang Zhao, Benlin Liu, Jiwen Lu, Jie Zhou, and Cho-Jui Hsieh. Dynamicvit: Efficient vision transformers with dynamic token sparsification. In M. Ranzato, A. Beygelzimer, Y. Dauphin, P.S. Liang, and J. Wortman Vaughan, editors, *Advances in Neural Information Processing Systems*, volume 34, pages 13937–13949. Curran Associates, Inc., 2021. URL https://proceedings.neurips.cc/paper_files/paper/2021/file/747d3443e319a22747fbb873e8b2f9f2-Paper.pdf.
- Michael Ryoo, AJ Piergiovanni, Anurag Arnab, Mostafa Dehghani, and Anelia Angelova. Tokenlearner: Adaptive space-time tokenization for videos. In M. Ranzato, A. Beygelzimer, Y. Dauphin, P.S. Liang, and J. Wortman Vaughan, editors, *Advances in Neural Information Processing Systems*, volume 34, pages 12786–12797. Curran Associates, Inc., 2021. URL https://proceedings.neurips.cc/paper_files/paper/2021/file/6a30e32e56fce5cf381895dfe6ca7b6f-Paper.pdf.
- Novendra Setyawan, Chi-Chia Sun, Mao-Hsiu Hsu, Wen-Kai Kuo, and Jun-Wei Hsieh. Microvit: A vision transformer with low complexity self attention for edge device, 2025. URL <https://arxiv.org/abs/2502.05800>.
- Hans Thisanke, Chamli Deshan, Kavindu Chamith, Sachith Seneviratne, Rajith Vidanaarachchi, and Damayanthi Herath. Semantic segmentation using vision transformers: A survey. *Engineering Applications of Artificial Intelligence*, 126:106669, 2023. ISSN 0952-1976. doi: <https://doi.org/10.1016/j.engappai.2023.106669>. URL <https://www.sciencedirect.com/science/article/pii/S0952197623008539>.
- Hugo Touvron, Matthieu Cord, Matthijs Douze, Francisco Massa, Alexandre Sablayrolles, and Herve Jegou. Training data-efficient image transformers & distillation through attention. In Marina Meila and Tong Zhang, editors, *Proceedings of the 38th International Conference on Machine Learning*, volume 139 of *Proceedings of Machine Learning Research*, pages 10347–10357. PMLR, 18–24 Jul 2021. URL <https://proceedings.mlr.press/v139/touvron21a.html>.

- Ashish Vaswani, Noam Shazeer, Niki Parmar, Jakob Uszkoreit, Llion Jones, Aidan N Gomez, Łukasz Kaiser, and Illia Polosukhin. Attention is all you need. In *Advances in Neural Information Processing Systems*, volume 30, 2017.
- Sinong Wang, Belinda Z. Li, Madian Khabsa, Han Fang, and Hao Ma. Linformer: Self-attention with linear complexity. *CoRR*, abs/2006.04768, 2020. URL <https://arxiv.org/abs/2006.04768>.
- Yaoli Wang, Yaojun Deng, Yuanjin Zheng, Pratik Chattopadhyay, and Lipo Wang. Vision transformers for image classification: A comparative survey. *Technologies*, 13(1), 2025. ISSN 2227-7080. doi: 10.3390/technologies13010032. URL <https://www.mdpi.com/2227-7080/13/1/32>.
- Han Xiao, Kashif Rasul, and Roland Vollgraf. Fashion-mnist: a novel image dataset for benchmarking machine learning algorithms. 08 2017. doi: 10.48550/arXiv.1708.07747.
- Enze Xie, Wenhai Wang, Zhiding Yu, Anima Anandkumar, Jose M. Alvarez, and Ping Luo. Segformer: Simple and efficient design for semantic segmentation with transformers. In M. Ranzato, A. Beygelzimer, Y. Dauphin, P.S. Liang, and J. Wortman Vaughan, editors, *Advances in Neural Information Processing Systems*, volume 34, pages 12077–12090. Curran Associates, Inc., 2021. URL https://proceedings.neurips.cc/paper_files/paper/2021/file/64f1f27bf1b4ec22924fd0acb550c235-Paper.pdf.
- Yunyang Xiong, Zhanpeng Zeng, Rudrasis Chakraborty, Mingxing Tan, Glenn Fung, Yin Li, and Vikas Singh. Nyströmformer: A nyström-based algorithm for approximating self-attention. *Proceedings of the AAAI Conference on Artificial Intelligence*, 35(16):14138–14148, May 2021. doi: 10.1609/aaai.v35i16.17664. URL <https://ojs.aaai.org/index.php/AAAI/article/view/17664>.
- Chenglin Yang, Yilin Wang, Jianming Zhang, He Zhang, Zijun Wei, Zhe Lin, and Alan Yuille. Lite vision transformer with enhanced self-attention. In *2022 IEEE/CVF Conference on Computer Vision and Pattern Recognition (CVPR)*, pages 11988–11998, 2022. doi: 10.1109/CVPR52688.2022.01169.
- Zhilin Yang, Zihang Dai, Yiming Yang, Jaime Carbonell, Russ R Salakhutdinov, and Quoc V Le. Xlnet: Generalized autoregressive pretraining for language understanding. In H. Wallach, H. Larochelle, A. Beygelzimer, F. d'Alché-Buc, E. Fox, and R. Garnett, editors, *Advances in Neural Information Processing Systems*, volume 32. Curran Associates, Inc., 2019. URL https://proceedings.neurips.cc/paper_files/paper/2019/file/dc6a7e655d7e5840e66733e9ee67cc69-Paper.pdf.
- Jing Yao, Bing Zhang, Chenyu Li, Danfeng Hong, and Jocelyn Chanussot. Extended vision transformer (exvit) for land use and land cover classification: A multimodal deep learning framework. *IEEE Transactions on Geoscience and Remote Sensing*, 61:1–15, 2023. doi: 10.1109/TGRS.2023.3284671.
- Haoran You, Huihong Shi, Yipin Guo, and Yingyan Lin. Shiftaddvit: Mixture of multiplication primitives towards efficient vision transformer. In A. Oh, T. Naumann, A. Globerson, K. Saenko, M. Hardt, and S. Levine, editors, *Advances in Neural Information Processing Systems*, volume 36, pages 33319–33337. Curran Associates, Inc., 2023. URL https://proceedings.neurips.cc/paper_files/paper/2023/file/69c49f75ca31620f1f0d38093d9f3d9b-Paper-Conference.pdf.
- Weihao Yu, Mi Luo, Pan Zhou, Chenyang Si, Yichen Zhou, Xinchao Wang, Jiashi Feng, and Shuicheng Yan. Metaformer is actually what you need for vision. In *2022 IEEE/CVF Conference on Computer Vision and Pattern Recognition (CVPR)*, pages 10809–10819, 2022. doi: 10.1109/CVPR52688.2022.01055.
- Li Yuan, Yunpeng Chen, Tao Wang, Weihao Yu, Yujun Shi, Zihang Jiang, Francis E. H. Tay, Jiashi Feng, and Shuicheng Yan. Tokens-to-token vit: Training vision transformers from scratch on imagenet. In *2021 IEEE/CVF International Conference on Computer Vision (ICCV)*, pages 538–547, 2021. doi: 10.1109/ICCV48922.2021.00060.

- YUHUI YUAN, Rao Fu, Lang Huang, Weihong Lin, Chao Zhang, Xilin Chen, and Jingdong Wang. Hrformer: High-resolution vision transformer for dense predict. In M. Ranzato, A. Beygelzimer, Y. Dauphin, P.S. Liang, and J. Wortman Vaughan, editors, *Advances in Neural Information Processing Systems*, volume 34, pages 7281–7293. Curran Associates, Inc., 2021. URL https://proceedings.neurips.cc/paper_files/paper/2021/file/3bbfdde8842a5c44a0323518eec97cbe-Paper.pdf.
- Chong Zhang, Jie Yue, Jianglong Fu, and Shouluan Wu. River floating object detection with transformer model in real time. *Scientific Reports*, 15(1):9026, Mar 2025. ISSN 2045-2322. doi: 10.1038/s41598-025-93659-1. URL <https://doi.org/10.1038/s41598-025-93659-1>.
- Yian Zhao, Wenyu Lv, Shangliang Xu, Jinman Wei, Guanzhong Wang, Qingqing Dang, Yi Liu, and Jie Chen. Detsr beat yolos on real-time object detection. In *2024 IEEE/CVF Conference on Computer Vision and Pattern Recognition (CVPR)*, pages 16965–16974, 2024. doi: 10.1109/CVPR52733.2024.01605.
- Sixiao Zheng, Jiachen Lu, Hengshuang Zhao, Xiatian Zhu, Zekun Luo, Yabiao Wang, Yanwei Fu, Jianfeng Feng, Tao Xiang, Philip H.S. Torr, and Li Zhang. Rethinking semantic segmentation from a sequence-to-sequence perspective with transformers. In *2021 IEEE/CVF Conference on Computer Vision and Pattern Recognition (CVPR)*, pages 6877–6886, 2021. doi: 10.1109/CVPR46437.2021.00681.
- Alex Zihao Zhu, Jieru Mei, Siyuan Qiao, Hang Yan, Yukun Zhu, Liang-Chieh Chen, and Henrik Kretschmar. Superpixel transformers for efficient semantic segmentation. In *2023 IEEE/RSJ International Conference on Intelligent Robots and Systems (IROS)*, pages 7651–7658, 2023. doi: 10.1109/IROS55552.2023.10341519.

Appendix

Superpixel Segmentation

- **Purpose:** Create regions that group similar pixels (e.g., all the pixels in a dog's fur) instead of chopping the image blindly.
- **How:** We use the SLIC algorithm, which balances color similarity and spatial closeness.
- **Math:** For an image $I \in \mathbb{R}^{H \times W \times C}$ (height H , width W , channels $C = 3$ for RGB), SLIC splits it into R superpixels:

$$\mathcal{S}(I) = \{S_1, S_2, \dots, S_R\},$$

where:

- $\bigcup_{r=1}^R S_r = I$ (covers the whole image),
- $S_i \cap S_j = \emptyset$ if $i \neq j$ (no overlap),
- R is small (e.g., 16 instead of 3136).
- **SLIC Details:**

Algorithm 3 SLIC Superpixel Segmentation

```
1: procedure SLIC( $I, K, \alpha = 0.1, \text{max\_iter} = 10$ )
2:   Convert to CIELAB color space:  $L \leftarrow \text{rgb2lab}(I)$   $\triangleright$  Better for human-like color perception
3:   Set grid spacing:  $S \leftarrow \sqrt{\frac{H \times W}{K}}$   $\triangleright$  Start with  $K$  rough clusters
4:   Place cluster centers  $\mathbf{C}$  on a grid spaced by  $S$ 
5:   for each iteration up to  $\text{max\_iter}$  do
6:     for each pixel  $(x, y)$  do
7:       Color distance:  $d_c = \|L(y, x) - L(c_y, c_x)\|_2$   $\triangleright$  How different in color?
8:       Spatial distance:  $d_s = \sqrt{(x - c_x)^2 + (y - c_y)^2}$   $\triangleright$  How far apart?
9:       Total distance:  $D = \sqrt{\left(\frac{d_c}{\max_c}\right)^2 + \left(\frac{d_s}{\alpha S}\right)^2}$   $\triangleright$  Blend with compactness  $\alpha$ 
10:      Assign pixel to the closest center based on  $D$ 
11:     end for
12:     Update centers to the average position/color of assigned pixels
13:   end for
14:   return Superpixel map  $\mathcal{S}$ 
15: end procedure
```

- K is the target number of superpixels (we pick 16).
- $\alpha = 0.1$ makes superpixels hug image edges tightly (low compactness).

Patch-to-Superpixel Mapping

- **Purpose:** Connect the old fixed patches to our new superpixels.
- **How:** For each patch, see which superpixel most of its pixels belong to.
- **Math:** If $\mathcal{X} = \{x_1, x_2, \dots, x_N\}$ are the patches (still 3136 of them), assign each x_i to a superpixel:

Algorithm 4 Patch-to-Superpixel Mapping

```

1: procedure PATCHTOSUPERPIXELMAP( $\mathcal{X}, \mathcal{S}$ )
2:   for each patch  $x_i \in \mathcal{X}$  do
3:     Get pixel coordinates in  $x_i$ :  $\mathcal{P}_i$ 
4:     Count labels:  $\mathbf{counts}_r = \sum_{p \in \mathcal{P}_i} \mathbf{1}_{\mathcal{S}(p)=r}$  ▷ How many pixels in superpixel  $r$ ?
5:     Assign:  $\mathbf{s}_i = \arg \max_r \mathbf{counts}_r$  ▷ Pick the winner
6:   end for
7:   return Mapping  $\mathbf{S} = \{\mathbf{s}_1, \dots, \mathbf{s}_N\}$ , where  $\mathbf{s}_i \in \{1, \dots, R\}$ 
8: end procedure

```

Adaptive Pooling

- **Purpose:** Merge all patches in a superpixel into one token, slashing the count from N to R .

- **Math:** Start with patch embeddings $\mathcal{E} = \{E_1, E_2, \dots, E_N\}$, where $E_i \in \mathbb{R}^D$ (e.g., $D = 768$).

For each superpixel r :

$$Q_r = \frac{1}{|\mathcal{I}_r|} \sum_{i \in \mathcal{I}_r} E_i,$$

Algorithm 5 Adaptive Pooling for Superpixels

```

1: procedure ADAPTIVEPOOLING( $\mathcal{E}, \mathcal{S}$ )
2:   Input: Patch embeddings  $\mathcal{E} = \{E_1, E_2, \dots, E_N\}$  where  $E_i \in \mathbb{R}^D$ , and superpixel map  $\mathcal{S} = \{S_1, S_2, \dots, S_R\}$ .
3:   Output: Reduced set of tokens  $\mathcal{Q} = \{Q_1, Q_2, \dots, Q_R\}$ .
4:   Initialize an empty list for pooled tokens:  $\mathcal{Q} \leftarrow []$ 
5:   for each superpixel  $r \in \{1, 2, \dots, R\}$  do
6:     Identify the indices of patches belonging to superpixel  $r$ :

```

$$\mathcal{I}_r = \{i \mid \mathbf{s}_i = r\}.$$

```

7:     Compute the average embedding for patches in  $\mathcal{I}_r$ :

```

$$Q_r = \frac{1}{|\mathcal{I}_r|} \sum_{i \in \mathcal{I}_r} E_i,$$

where $|\mathcal{I}_r|$ is the number of patches in superpixel r .

```

8:     Add  $Q_r$  to the list of pooled tokens:  $\mathcal{Q} \leftarrow \mathcal{Q} \cup \{Q_r\}$ 
9:   end for
10:  return Pooled tokens  $\mathcal{Q}$ 
11: end procedure

```

Dynamic Positional Encoding (PE)

- **Purpose:** Tell the transformer where each superpixel is, since fixed grid positions don't fit anymore.

- **Math:** Compute the centroid of superpixel S_r :

$$c_x^r = \frac{1}{|S_r|} \sum_{(x,y) \in S_r} x, \quad c_y^r = \frac{1}{|S_r|} \sum_{(x,y) \in S_r} y,$$

then:

$$PE_r = \text{MLP} \left(\frac{c_x^r}{W}, \frac{c_y^r}{H} \right) \in \mathbb{R}^D,$$

Algorithm 6 Dynamic Positional Encoding for Superpixels

```

1: procedure DYNAMICPOSITIONALENCODING( $\mathcal{S}, H, W, D$ )
2:   Input: Superpixel map  $\mathcal{S} = \{S_1, S_2, \dots, S_R\}$ , image height  $H$ , image width  $W$ , embedding
   dimension  $D$ .
3:   Output: Positional encodings  $\mathcal{P} = \{PE_1, PE_2, \dots, PE_R\}$ .
4:   Initialize an empty list for positional encodings:  $\mathcal{P} \leftarrow []$ 
5:   for each superpixel  $r \in \{1, 2, \dots, R\}$  do
6:     Compute the centroid of superpixel  $S_r$ :

$$c_x^r = \frac{1}{|S_r|} \sum_{(x,y) \in S_r} x, \quad c_y^r = \frac{1}{|S_r|} \sum_{(x,y) \in S_r} y,$$

       where  $|S_r|$  is the number of pixels in superpixel  $S_r$ .
7:     Normalize the centroid coordinates to  $[0, 1]$ :

$$\hat{c}_x^r = \frac{c_x^r}{W}, \quad \hat{c}_y^r = \frac{c_y^r}{H}.$$

8:     Pass the normalized coordinates through an MLP to compute the positional encoding:

$$PE_r = \text{MLP}(\hat{c}_x^r, \hat{c}_y^r) \in \mathbb{R}^D.$$

9:     Add  $PE_r$  to the list of positional encodings:  $\mathcal{P} \leftarrow \mathcal{P} \cup \{PE_r\}$ 
10:  end for
11:  return Positional encodings  $\mathcal{P}$ 
12: end procedure

```

Full Workflow

Here’s how it all ties together:

Algorithm 7 SPPP-Modified ViT Workflow

```

1: procedure SPPPViT( $I, K, \alpha$ , Transformer)
2:    $\mathcal{S} \leftarrow \text{SLIC}(I, K, \alpha)$  ▷ Make superpixels
3:    $\mathcal{X} \leftarrow \text{Patchify}(I)$  ▷ Get fixed patches
4:    $\mathbf{S} \leftarrow \text{PatchToSuperpixelMap}(\mathcal{X}, \mathcal{S})$  ▷ Link patches to superpixels
5:    $\mathcal{Z} \leftarrow \text{AdaptivePooling}(\mathcal{X}, \mathbf{S})$  ▷ Pool into fewer tokens
6:    $\mathcal{Z}_{\text{PE}} \leftarrow \text{DynamicPositionalEncoding}(\mathcal{S})$  ▷ Add position info
7:    $\hat{y} \leftarrow \text{Transformer}(\mathcal{Z}_{\text{PE}})$  ▷ Run ViT
8:   return  $\hat{y}$  ▷ Prediction
9: end procedure

```

Comparison to Traditional ViT

Step	Traditional ViT	ViT + SPPP
Patch Generation	Fixed grid (e.g., 4×4)	Fixed grid, then superpixels
Token Count	$N = (H/P)^2 = 3136$	$R = 16$
Positional Encoding	Fixed grid	Dynamic, superpixel-based
Self-Attention Complexity	$\mathcal{O}(3136^2)$	$\mathcal{O}(16^2)$

Table 6: How SPPP Changes ViT

Mathematical Formulation

Why Does It Work? This section digs into the math behind SPPP to show why it’s effective.

Superpixel Segmentation

- **Definition:** A superpixel S_r is a group of pixels that look similar and are close together.

Formally:

$$\mathcal{S}(I) = \{S_1, S_2, \dots, S_R\},$$

with $\bigcup_{r=1}^R S_r = I$ and no overlap between them.

Patch Embedding and Pooling

- **Standard ViT:** Splits the image into:

$$\mathcal{P}(I) = \{P_1, P_2, \dots, P_N\}, \quad N = \frac{H \times W}{P^2},$$

then embeds each P_i into E_i .

- **SPPP:** Takes those E_i 's and pools them into Q_r 's, reducing N to R .

Patch-to-Superpixel Mapping

- **Math:** Each patch P_i picks its superpixel by:

$$s_i = \arg \max_r \frac{|\{p \in P_i \mid p \in S_r\}|}{|P_i|},$$

counting how many of its pixels fall in each S_r .

Signal-to-Noise Ratio (SNR) Enhancement

- **Why Pooling Helps:** Combining patches reduces noise.

- **Theorem:** If $E_i = s + n_i$ (signal s , noise $n_i \sim \mathcal{N}(0, \sigma^2)$), then:

$$Q_r = \frac{1}{m} \sum_{i=1}^m E_i, \quad m = |\mathcal{I}_r|,$$

and:

$$\text{SNR}(Q_r) = m \cdot \text{SNR}(E_i).$$

Proof:

- Noise in Q_r : $\frac{1}{m} \sum n_i$,

- Variance: $\text{Var}(Q_r) = \frac{1}{m^2} \cdot m \cdot \sigma^2 = \frac{\sigma^2}{m}$,

- SNR: $\frac{s^2}{\sigma^2/m} = m \cdot \frac{s^2}{\sigma^2}$.

- Result: Noise drops, signal stays, making tokens clearer.

Complexity Analysis

- **Lemma:** Self-attention goes from $\mathcal{O}(N^2)$ to $\mathcal{O}(R^2)$.

- **Speedup:** $\left(\frac{N}{R}\right)^2 = \left(\frac{3136}{16}\right)^2 = 196^2 = 38416$, or about 34,000× faster attention.

Token Embedding Comparison

- **Base ViT:** $X_{\text{base}} = [E_{\text{cls}}, E_1, \dots, E_N]$, size (3137×768) .

- **SPPP-ViT:** $X_{\text{sppp}} = [E_{\text{cls}}, Q_1, \dots, Q_R]$, size (17×768) .

Table 7: Comparison of various datasets used in the study.

Dataset	Image Dimensions	No. of Classes	Train Set	Test Set
CIFAR-10	32×32	10	50k	10k
CIFAR-100	32×32	100	50k	10k
SVHN	32×32	10	73.2k	26k
Fashion MNIST	28×28	10	60k	10k
STL10	96×96	10	5k	8k